RSC Advances

PAPER

View Article Online
View Journal | View Issue

Cite this: *RSC Adv.*, 2023, **13**, 25360

Directing the size and dispersity of silver nanoparticles with kudzu leaf extracts†

Jaley Faith Adkins,[a] Amandeep Kaur,[a] Md. Sofiul Alom,[a] Haridas Chandran,[b] Farshid Ramezanipour[a] and Andrew J. Wilson *[a]

Kudzu is an abundant and invasive species in the Southeastern United States. The prospective use of kudzu as a non-toxic, green and biocompatible reducing and stabilizing agent for one-pot Ag nanoparticle synthesis was investigated. Ag nanoparticles were synthesized using aqueous and ethanolic kudzu leaf and stem extracts. The size and dispersity of the synthesized nanoparticles were found to depend on the extract used. Ultraviolet-visible and Fourier transform infrared spectroscopies were used to characterize the extracts. Surface-enhanced fluorescence and Raman scattering were used to characterize the surface species on synthesized Ag nanoparticles. The primary reducing and stabilizing agents in aqueous kudzu leaf extracts were determined to be reducing sugars and saponins which result in Ag nanoparticles with average diameters of 21.2 ± 4.8 nm. Ethanolic kudzu leaf extract was determined to be composed of chlorophyll, reducing sugars and saponins, producing Ag nanoparticles with average diameters of 9.0 ± 1.6 nm. Control experiments using a chlorophyllin standard as the reducing and stabilizing agent reveal that chlorophyll has a key role in the formation of small and monodisperse Ag nanoparticles. Experiments carried out in the absence of light demonstrate that reducing sugars and saponins also contribute to the formation of Ag nanoparticles in ethanolic kudzu leaf extracts. We propose a mechanism by which reducing sugars donate electrons to reduce Ag^+ leading to the formation of Ag nanoparticles, forming carboxylic acid sugars which stabilize and partially stabilize Ag nanoparticles synthesized with aqueous and ethanolic kudzu leaf extracts, respectively. In the ethanolic extract, photoexcited chlorophyll serves as a co-reducing and co-stabilizing agent, leading to small and monodisperse Ag nanoparticles.

Received 8th June 2023
Accepted 3rd August 2023

DOI: 10.1039/d3ra03847e

rsc.li/rsc-advances

Introduction

Ag nanoparticles have been widely explored for and employed in health applications such as pharmaceuticals, therapeutics, drug delivery vehicles, cosmetics, wound healing, and used as antimicrobial agents.[1–11] The green synthesis of Ag nanoparticles using plant extracts is an important strategy to circumvent the use of toxic reducing and stabilizing agents and impart biocompatibility to the nanoparticles.[12–14] Numerous plant species have been used to create extraction mixtures which form Ag nanoparticles of various morphologies and sizes.[14] In addition to surface modification, the average diameter and distribution of diameters of a population of nanoparticles are vital for circulation within and elimination from biological entities as well as for accurate diagnostics.[15,16] Nanoparticle morphology is also an important physical trait that can be leveraged to enhance diagnostics and antimicrobial activity.[17,18] Although different parts of plants (*e.g.*, leaves, stems, flowers) and different plant species have produced a range of nanoparticle morphologies, sizes, and dispersity, control over these attributes is a challenge when using plant extracts to synthesize Ag nanoparticles.

Several reviews highlight the diversity of plant species that can be used in the green synthesis of Ag nanoparticles.[12–14] The chemical compositions of plant extracts vary widely and have a marked impact on the morphology and size of Ag nanoparticles when used as reducing and stabilizing agents. A primary challenge in understanding how to use plant extracts for the controlled synthesis of Ag nanoparticles is the identification of chemical species in the extract and evaluating their role in the synthetic procedure. Biomolecules often cited as reducing and stabilizing agents include carboxylic acids, flavonoids, polyphenolic compounds and polysaccharides, among others.[14,19,20] Knowing the precise identity and concentration of reducing and stabilizing agents, as well as assaying reaction conditions to synthesize Ag nanoparticles, would enable synthetic design rules to be established for targeted applications.

[a]*Department of Chemistry, University of Louisville, Louisville, Kentucky, 40292, USA. E-mail: aj.wilson@louisville.edu*

[b]*Belfry High School, Belfry, Kentucky, 41514, USA*

† Electronic supplementary information (ESI) available. See DOI: https://doi.org/10.1039/d3ra03847e

A plant species that has not been used in the synthesis of Ag nanoparticles is kudzu (*Pueraria montana* var. *lobata*). As an invasive plant species, kudzu is responsible for a biogeochemical nitrogen fixing process that suffocates surrounding plants.[21] This plant has been spreading across the Southern and Southeastern United States since its introduction in 1876, covering three million hectares and spreading 50 000 hectares per year.[22] On the other hand, kudzu has a long history of use in herbal medicine, dating back over 2000 years in China, with its roots being used to treat a range of ailments from diabetes to cardiovascular disease.[23] The leaves of the plant have also been shown to have health benefits stemming from the robinin present that helps to decrease inducible nitric oxide synthase protein, which contributes to modulation of c-Jun N-terminal kinase and transcription 1 activation, serving to reduce inflammation.[24] The abundance and known health benefits make kudzu a strong candidate to serve as a reducing and stabilizing agent in the green synthesis of biocompatible Ag nanoparticles.

In this study, kudzu extract was used to reduce Ag^+ and stabilize Ag nanoparticles in a one-pot synthesis. Kudzu leaf and stem extracts were prepared using water and ethanol as extraction solvents and characterized with ultraviolet (UV)-visible spectroscopy, Fourier transform infrared (FTIR) spectroscopy, and thin-layer chromatography (TLC). The formation of Ag nanoparticles in the presence of kudzu extracts was evaluated by measuring localized surface plasmon resonances, transmission electron microscopy (TEM) images of Ag nanoparticles, powder X-ray diffraction and surface-enhanced spectroscopy. Ethanolic kudzu leaf extracts formed small and monodisperse Ag nanoparticles compared to aqueous leaf or stem extracts. Control experiments synthesizing Ag nanoparticles with chlorophyllin standards and kudzu leaf extracts in dark conditions revealed that chlorophyll plays a major role in the synthesis of small and monodisperse Ag nanoparticles. Reducing sugars and saponins are suspected to serve as the co-reducing and co-stabilizing agents in ethanolic kudzu leaf extracts, having a secondary role in the synthesis of small and monodisperse Ag nanoparticles. By contrast, reducing sugars and saponins are primary reducing and stabilizing agents in aqueous extracts, leading to larger and more disperse Ag nanoparticles sizes.

Experimental

Chemicals

Silver nitrate ($AgNO_3$, 99%, lot #22C0256162), sulfuric acid (lot #2020081109), methanol (lot #0000265583), chloroform (lot #21J1456829), isopropanol (lot #22K1561065), and hexane (lot #0000258628) were purchased from VWR. Ethanol (Supelco, 200 proof, lot #62154), Dragendorff reagent (lot #BCBX4809), trisodium citrate dihydrate (lot #SLCP1502), copper(II) sulphate (lot #MKCR0607), hydrochloric acid (lot #MKCN0724), and iron(III) chloride (lot #STBK8949) were purchased from Millipore Sigma. Sodium copper chlorophyllin (lot #AD-22021) was purchased from Ward's Science. Acetone was purchased from Fisher Scientific. Potassium carbonate (lot #50019773) was purchased from BeanTown Chemical. Mg chips (lot #35695600) were purchased from Stream Chemicals. Water (H_2O, 18.2 MΩ cm) was obtained from a water purification system (Sartorius, Arium mini).

Kudzu extract preparation

Kudzu leaves and stems were harvested from the Appalachian Mountains in Canada, Kentucky and placed into a food dehydrator for a minimum of 24 h, or until the leaves (stems) were brittle. A mortar and pestle were used to crush the dried leaves (stems) into powder form. The powdered leaves (stems) were used to create extracts using either water or ethanol as the extraction solvent.

To prepare water-based extracts, 100 mL of water was placed into a 250 mL beaker with a stir bar and heated on a hot plate for 15 min to bring the water to a gentle boil. Next, 1.0 g of leaf (stem) powder was added, and the suspension was boiled for an additional 60 min. After boiling, the suspension was cooled to room temperature and gravity filtered twice using Whatman 90 mm filter paper (lot no. 16976613). The final aqueous extract volume was diluted to the original volume of 100 mL.

Ethanol-based extracts were prepared by boiling a kudzu leaf (stem) suspension under reflux conditions. 100 mL of ethanol was placed into a 250 mL round-bottom flask and heated *via* a water bath for 15 min before the addition of 1.0 g of kudzu leaves (stems). The suspension was boiled for an additional 60 min. After boiling, the suspension was cooled to room temperature and filtered by centrifugation at 1137 *g* for 30 min using an IEC clinical centrifuge to obtain the extract. The final ethanolic extract volume was diluted to the original volume of 100 mL. Aqueous and ethanolic extracts were stored in a refrigerator until used in the synthesis of Ag nanoparticles.

Chlorophyllin standards

Chlorophyllin standards were prepared by dissolving 1.0 g of chlorophyllin in 100 mL of water or ethanol under boiling conditions as described in the extract preparation. The chlorophyllin standards were diluted 100× to decrease the concentration to be representative of the amount of chlorophyll found in the ethanolic kudzu extract as determined by UV-visible spectroscopy.

Extract characterization

Extracts were characterized using an Agilent Cary 60 UV-visible spectrophotometer, an Agilent Cary 630 FTIR instrument, and TLC. UV-visible absorbance spectra were acquired in quartz cuvettes from aqueous and ethanolic extracts diluted 25× and 8.3×, respectively. FTIR spectra were obtained from solid samples to eliminate solvent interference. Solids from the extracts were collected by rotary evaporation of the solvent.

TLC was performed using a mobile phase composition of 3 mL of acetone and 6 mL of hexane, and a silica-covered glass plate as the stationary phase. The mobile phase was put into a 200 mL beaker and covered with a watch glass. The glass plate was marked with a pencil one cm from the top and bottom. A pipette was used to add drops of each extract one cm from the bottom of the plate. The extract was given 2 min to dry on the

plate before being placed into the beaker with the mobile phase and being covered with a watch glass. The glass plate was removed when the mobile phase reached one cm from the top of the plate and the spots left by the extracts were marked to determine retention factors.

Phytochemical profile of kudzu leaves and extract

The presence of reducing sugars, alkaloids, flavonoids, steroids, terpenoids, saponins, and tannins in kudzu leaves, aqueous kudzu leaf extracts, and ethanolic kudzu leaf extracts were determined by the phytochemical screening tests described below.[25–27]

Reducing sugars. 100 mg of dried leaf powder or 1 mL of extract was added to a 2 mL solution containing 0.7 M potassium carbonate, 0.7 M trisodium citrate, and 0.07 M copper(II) sulphate pentahydrate. The solution prepared with the leaf powder was then filtered. Each solution was next heated in a boiling water bath for 5 minutes. A colour change from blue to green indicated the presence of reducing sugars.

Alkaloids. 20 mg of dried leaf powder or 0.02 mL of extract was stirred with 1% HCl in a heated water bath. The solution prepared with the leaf powder was then filtered. To each solution, 7–8 drops of Dragendorff reagent was added. No orange to red coloured precipitate was formed indicating the absence of alkaloids.

Flavonoids. 1 mL of methanol was used to dissolve 20 mg of dried leaf powder or mixed with 0.02 mL of extract. The solution prepared with the leaf powder was then filtered. A magnesium chip and 7–8 drops of 11.6 M HCl were added to each solution sequentially. The solutions did not change to a magenta colour which indicates no flavonoids are present.

Steroids. 2 mL of chloroform was used to dissolve 20 mg of dried leaf powder or mixed with 0.02 mL of extract. The solution prepared with the leaf powder was then filtered. To each solution, 10 drops of concentrated sulfuric acid were added. A brown chloroform layer formed indicating the presence of steroids in kudzu leaves.

Terpenoids. 20 mg of dried leaf powder or 0.02 mL of extract was added to 2 mL of methanol. The solution prepared with the leaf powder was then filtered. 2 mL of concentrated sulfuric acid was added, and the solutions were shaken. A brown precipitate was not formed indicating the absence of terpenoids.

Saponins. 500 mg of dried leaf power or 0.5 mL of extract was added to 15 mL of deionized water. The solution prepared with the leaf powder was then filtered. Each solution was shaken vigorously for 5 min. A stable froth on top of the solution indicated the presence of saponins.

Tannins. 20 mg of dried leaf powder or 0.02 mL of extract was added to 2 mL of deionized water. The solution prepared with the leaf powder was then filtered. 7–8 drops of 1% ferric chloride solution were added. The absence of a blue colour indicated there are no tannins present in the samples.

Ag nanoparticle synthesis

To synthesize Ag nanoparticles, 150 mL of water, 1.5 mL of 0.04 M $AgNO_3$ (final reaction concentration of 0.33 mM) and a stir bar were placed into a 250 mL Erlenmeyer flask and put on a hot plate for 15 min to bring the solution to a gentle boil. When the solution began to boil, 30 mL of kudzu leaf extract (final reaction concentration of 16.5% v/v) or 100× diluted chlorophyllin standard was added, and the solution was continually boiled for an additional 60 min. Nanoparticle formation resulted in a colour change of the solution (Fig. S1†). After boiling, the solution was allowed to cool for 15 min and then diluted with water to a final volume of 181.5 mL. Nanoparticle syntheses were carried out in triplicate for each set of reaction conditions. Unless otherwise noted, all nanoparticle syntheses were carried out under exposure to ambient room light. The final nanoparticle colloids were characterized with UV-visible spectroscopy and TEM (Hitachi HT7700) operated at 80 kV. Size determinations of Ag nanoparticles were performed in ImageJ. Nanoparticles sizes are reported as average values and the dispersity is reported as the standard deviation of the sizes.

Powder X-ray diffraction

Ag nanoparticle powders were prepared by evaporation of the solvent from synthesized Ag nanoparticle colloids. The formation of Ag nanoparticles was confirmed by high resolution powder X-ray diffraction (XRD) using $K\alpha_1$ radiation (λ = 1.540556 Å) on an Empyrean diffractometer equipped with a monochromator.

Surface-enhanced fluorescence and Raman scattering

Chemicals and functional groups on the surface of Ag nanoparticles were measured with surface-enhanced fluorescence and Raman scattering. Samples were prepared by drop-casting 10 μL of a Ag nanoparticle colloid onto glass coverslips (No. 1, VWR) cleaned by sequential sonication in isopropanol and deionized water. The colloid was allowed to dry in ambient air on a glass coverslip overnight. The glass coverslips with dried Ag nanoparticles were rinsed with either deionized water or ethanol (based on the extraction solvent used to synthesize the Ag nanoparticles) and dried with a stream of nitrogen gas. The samples were then mounted onto the stage of an inverted optical microscope (IX73 Olympus). 0.2 mW of a circularly polarized 532 nm laser (Oxxius LCX-532) was focused onto the drying ring of aggregated Ag nanoparticles using an oil-immersion 100× objective. Fluorescence or Raman scattering spectra were collected using a Teledyne Princeton Instruments spectrometer (IsoPlane SCT-300) and electron-multiplied charge-coupled device (PROHS1024BX3).

Results and discussion

The solvent used in the kudzu extraction process determines the chemical composition of the extract. In the aqueous kudzu leaf extract, narrow peaks at 265, 286, and 321 nm are observed in the UV-visible absorbance spectra (Fig. 1, red curve). The ethanolic kudzu leaf extract exhibits the same absorbance peak at 265 nm, but also has peaks at 340, 375, 415, 435, 464, 534, 615, and 665 nm (Fig. 1, blue curve). The electronic resonances

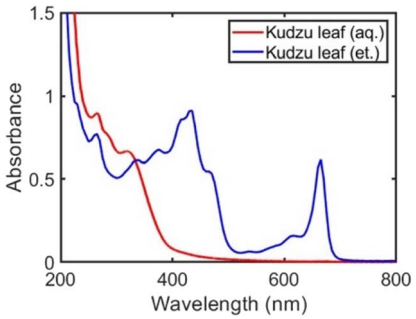

Fig. 1 UV-visible spectra of aqueous (red curve) and ethanolic (blue curve) kudzu leaf extracts.

of the ethanolic extract at 415, 534, 615, and 665 nm are attributed to the presence of chlorophyll a in the extract.[28–30] This is supported by absorbance spectra of aqueous and ethanolic chlorophyllin solutions (Fig. S2†), which contain similar porphyrin rings as found in chlorophyll. Chlorophyllin is a derivative of chlorophyll where Mg ions are replaced with Cu ions and the phytol chain is removed. The shoulder peaks at 435 and 464 nm suggest chlorophyll b is also present in the ethanolic extract.[28,29] The less polar solvent ethanol is more efficient in extracting relatively non-polar chlorophyll (due to the phytol chain) from kudzu leaves compared to water. Electronic resonances in the UV portion of the spectra of the extracts are likely associated with reducing sugars and saponins (discussed further below).[31–34] A mixture of ethanol and water produced extracts with components pertaining to the pure solvent extracts (Fig. S3†). The chemical composition of the kudzu leaf extracts was found to be stable over a five-day period (Fig. S4†). Extractions performed with kudzu stems and water were determined to have a chemical composition different than aqueous kudzu leaf extracts, but the concentration of extracted species was drastically lower as determined by low UV-visible absorbance values (Fig. S5†).

Ag nanoparticles were formed in a one-pot synthesis using the components of the kudzu extracts as reducing and capping agents. Due to the high concentration of extracted species and the largest difference in nanoparticle properties, we focus our study on Ag nanoparticles synthesized with kudzu leaf extracts prepared with either pure water or pure ethanol (Ag nanoparticles synthesized with stem extracts and solvent mixtures are shown in Fig. S6 and S7†).

Conditions for Ag nanoparticle synthesis were optimized using aqueous and ethanolic kudzu leaf extracts. The age of the extract (*i.e.*, time lapsed after the extraction process) did not affect the formation of Ag nanoparticles or their properties as determined by a reproducible plasmon resonance peak wavelength and linewidth (Fig. S8†). This observation is consistent with the observation that the chemical composition of the extracts did not vary over a five-day period as determined by UV-visible spectroscopy of the pure extract. Next, the final concentration of $AgNO_3$ and extract used in the synthesis of Ag nanoparticles was assayed between 33 μM–3.6 mM and 0.20–16.7% v/v, respectively. In general, an increase in the concentration of $AgNO_3$ and volume of the extract led to an increase in the number of Ag nanoparticles synthesized, evidenced by an increase in the extinction of the Ag nanoparticle plasmon resonance peak (Fig. S9 and S10†). However, $AgNO_3$ concentrations greater than 3.0 mM were determined to lead to the formation of aggregated nanoparticles due to a broad, red-shifted shoulder in the plasmon resonance peak of Ag nanoparticles. Therefore, we determined that 0.33 mM $AgNO_3$ and 16.5% v/v extract are conditions that maximize the number of individually stabilized Ag nanoparticles.

Under optimized reagent concentrations, Ag nanoparticles were synthesized with aqueous or ethanolic kudzu leaf extracts. Both extracts produced Ag nanoparticles as evidenced by a plasmon band in their UV-visible spectra that is distinct from the absorbance features of the isolated extracts (Fig. 2 and S11†). Ag nanoparticles synthesized with the aqueous and ethanolic kudzu leaf extracts exhibited a plasmon band with a peak wavelength of 410 nm. Post-synthesis, electronic resonances from the extracts were present indicating the chemical species in the extract are in excess. Of note is the resonance at 670 nm in the Ag nanoparticle colloid synthesized with the ethanolic extract, attributed to chlorophyll. The plasmon band of Ag nanoparticles synthesized with the aqueous kudzu leaf extract has a broad shoulder red-shifted of the resonance peak, indicative of a relatively large distribution of Ag nanoparticles sizes. By comparison, the plasmon band of Ag nanoparticles synthesized with the ethanolic extract is narrow, indicating a smaller distribution of Ag nanoparticle sizes. From optical characterization, we concluded that Ag nanoparticles synthesized with ethanolic kudzu leaf extracts have a narrower size distribution than Ag nanoparticles synthesized with aqueous kudzu leaf extracts.

Ag nanoparticles synthesized with aqueous or ethanolic kudzu leaf extracts were characterized with TEM (Fig. 3 and S12†) to substantiate our conclusions from UV-visible spectroscopy. The ethanolic extract produced spheroidal nanoparticles. The aqueous extract formed primarily spheroidal and ellipsoidal nanoparticles, along with a minority population of irregularly shaped nanoparticles. From a size analysis of 100 nanoparticles, the reducing/capping agents from ethanolic and aqueous extracts formed Ag nanoparticles with average diameters of 9.0 ± 1.6 nm and 21.2 ± 4.8 nm, respectively (Fig. 4).

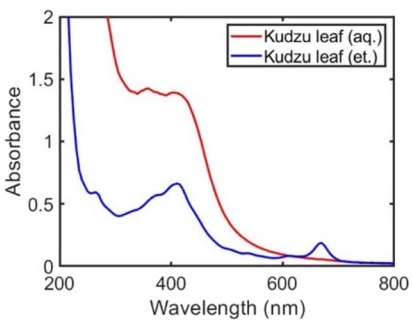

Fig. 2 UV-visible spectra of Ag nanoparticle colloids formed using aqueous (red curve) and ethanolic (blue curve) kudzu leaf extracts.

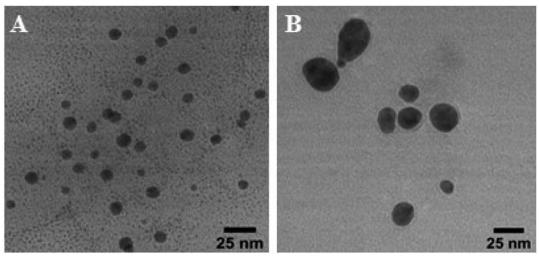

Fig. 3 Representative TEM images of Ag nanoparticles synthesized with (A) ethanolic and (B) aqueous kudzu leaf extracts.

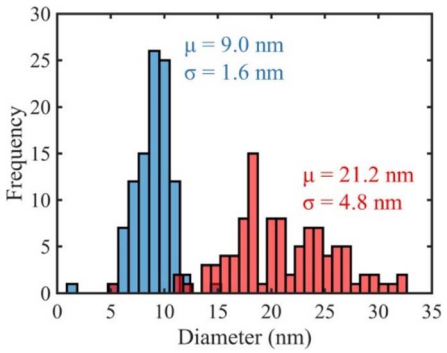

Fig. 4 Size histograms of Ag nanoparticles synthesized with aqueous (red) and ethanolic (blue) kudzu leaf extracts.

Ethanolic kudzu leaf extracts lead to the formation of smaller and more monodisperse Ag nanoparticles than aqueous extracts, desirable characteristics for sustainably synthesized and biocompatible Ag nanoparticles.[35]

To confirm the synthesized nanoparticles are Ag, we investigated the Ag nanoparticle powders using XRD. We observed diffraction peaks at $2\theta = 38.1°$, 44.3°, 64.5° and 77.4° from Ag nanoparticles prepared with the aqueous kudzu leaf extracts (Fig. 5 and S13†). Using a simulated powder XRD pattern, we assign these peaks to the (111), (200), (220) and (311) crystallographic planes of Ag, in agreement with literature reports.[36–38] Additional to these characteristic Ag peaks, diffraction patterns for the Ag nanoparticles, particularly those synthesized with the ethanolic extract, showed a prominent peak at 31.2° and smaller peaks at $2\theta \approx 21.8°$, 23.9°, 27.0°, 27.9°, 32.3°, 55.3° and 73.5° (Fig. S13†), likely due to unreacted and recrystallized $AgNO_3$. We note that $AgNO_3$ can crystalize with multiple different structures.[39–41] The full width at half maximum (fwhm) of the diffraction peak at $2\theta = 38.1°$ for Ag nanoparticles synthesized with the aqueous and ethanolic kudzu leaf extracts is 0.5° and 1.3°, respectively. Given the inverse relation between the fwhm and the particle size, the larger diffraction peak width of the Ag nanoparticles synthesized with the ethanolic extract is consistent with a population of smaller nanoparticles sizes.

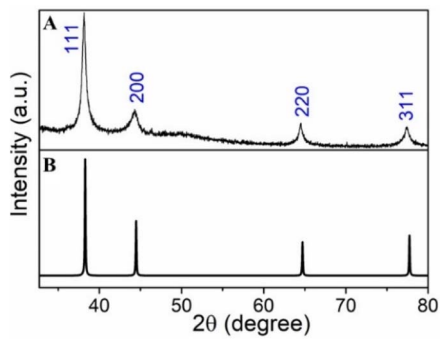

Fig. 5 (A) Experimental and (B) simulated powder X-ray diffraction data of Ag nanoparticles synthesized with the aqueous kudzu leaf extracts.

To understand why ethanolic kudzu leaf extracts produced smaller and more monodisperse Ag nanoparticles, we performed control experiments substituting the chemical mixture of the extracts with chlorophyllin. Based on the non-polar phytol chain of chlorophyll, and the UV-visible spectrum of the ethanolic extract, we expect chlorophyll to be extracted from kudzu leaves using ethanol as a solvent with little to no chlorophyll being extracted by water. Further, we expect that the charged porphyrin would act as a suitable stabilizing agent for Ag nanoparticles in an aqueous or ethanolic media. Therefore, by synthesizing Ag nanoparticles with chlorophyllin dissolved in ethanol or water, insight into the role of the reducing and stabilizing (*i.e.*, capping) agents can be deduced. Moreover, by maintaining the chemical composition of the standard, the role of ethanol in the synthesis of Ag nanoparticles can be evaluated.

Standards of chlorophyllin dissolved in ethanol or water showed similar features in their UV-visible absorbance spectra with small solvatochromic peak shifts (Fig. S2†). Likewise, Ag nanoparticles synthesized with an aqueous or ethanolic chlorophyllin standard supported plasmon resonances that appear as a shoulder of the chlorophyllin absorption feature at 402 nm

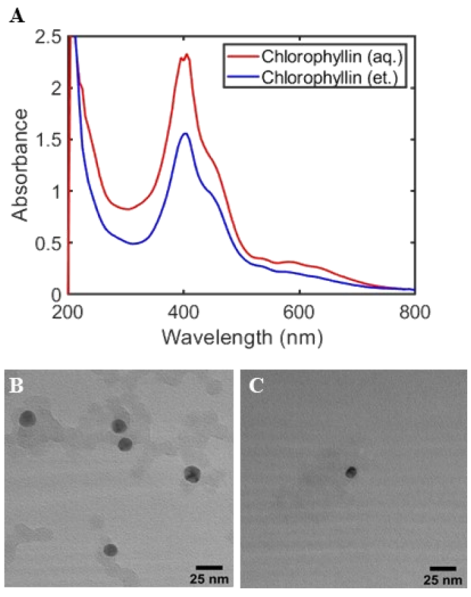

Fig. 6 (A) UV-visible spectra of Ag nanoparticles formed using an aqueous (red curve) and ethanolic (blue curve) chlorophyllin standard. Representative TEM images of Ag nanoparticles synthesized with an (B) ethanolic and (C) aqueous kudzu chlorophyllin standard.

(Fig. 6A). The overlap of the chlorophyllin peak and plasmon resonance prevents an accurate determination of the peak wavelength of the plasmon resonance, but the two nanoparticle populations are estimated to have similar dispersity due to the lack of a broad, red-shifted shoulder of the plasmon resonance. TEM images show that both solvents produce spheroidal nanoparticles (Fig. 6B and C). The average diameter of 100 Ag nanoparticles synthesized with the ethanolic chlorophyllin standard is 13.6 ± 2.1 nm. The aqueous chlorophyllin standard yielded significantly fewer Ag nanoparticles. From a limited sampling of 27 nanoparticles, the aqueous standard produced Ag nanoparticles with an average diameter of 10.2 ± 2.8 nm.

The formation of Ag nanoparticles in the presence of the chlorophyllin standards supports the hypothesis that the porphyrin ring of chlorophyll can serve as a reducing and stabilizing agent in the conversion of Ag^+ to Ag^0 and finally to Ag nanoparticles. The Ag nanoparticles synthesized with the chlorophyllin standards are much smaller in size than those synthesized with the aqueous kudzu leaf extract and similar in size to those synthesized with the ethanolic kudzu leaf extract. Further, the dispersity of the Ag nanoparticles synthesized with chlorophyllin, as determined by the standard deviation of the nanoparticle diameters about the mean, matches that of Ag nanoparticles synthesized with the ethanolic kudzu leaf extract. From the similar size and dispersity, we conclude that chlorophyll in the ethanolic kudzu leaf extract plays a major role in the synthesis of small and monodisperse Ag nanoparticles. The difference in the size of Ag nanoparticles synthesized with the ethanolic extract and chlorophyllin standards may be attributed to additional chemical species present in the ethanolic extract contributing to the reduction of Ag^+ and stabilization of Ag nanoparticles. The aqueous extract does not contain a high enough concentration of chlorophyll to produce small and relatively monodisperse Ag nanoparticles, but likely contains a wide mixture of chemical species that serve as reducing and stabilizing agents, leading to a larger range of nanoparticle sizes. Similarly, the kudzu stem extract does not contain chlorophyll and leads to a wide distribution of nanoparticle sizes as determined by a broad plasmon band (Fig. S6†). Ag nanoparticles synthesized with extract prepared with equal volumes of ethanol and water also have a broad size distribution (Fig. S7†).

The porphyrin ring in chlorophyll is known to absorb light, promoting an electron into an excited state, and form a highly reducing species. In photosynthesis, this electron is shuttled from photosystem II to photosystem I and the electrons are replenished by the oxidation of water.[42] The formation of Ag nanoparticles occurs in dark conditions when Ag^+ ions are heated in the presence of chlorophyll in the ethanolic kudzu leaf extract (Fig. S14†). The average diameter of 100 nanoparticles synthesized under these conditions is 12.1 ± 6.3 nm. Thus, photoexcited chlorophyll is not the only possible reducing agent in the ethanolic extract. However, in the presence of heat and light, the average nanoparticle diameter and distribution of diameters decreases, indicating that photoexcited chlorophyll plays a role in the final size of Ag nanoparticles and, more importantly, the distribution of sizes within a population of Ag nanoparticles. In the presence of light, photoexcited chlorophyll or chlorophyllin may transfer electrons to Ag^+ to form Ag^0, and subsequently, Ag nanoparticles are formed. The holes left behind either oxidize and decompose the reducing agent or are quenched by oxidation of the solvent. We note that ethanol has a lower oxidation potential than water, which improves the kinetics of Ag nanoparticle synthesis and likely contributes to the low dispersity of the Ag nanoparticles synthesized with the ethanolic kudzu leaf extract. This is also likely the reason that fewer Ag nanoparticles were formed using the aqueous chlorophyllin standard compared to the ethanolic chlorophyllin standard. Exposed to ambient light, chlorophyllin standards produced relatively monodisperse Ag nanoparticles with a slightly larger average diameter than ethanolic kudzu leaf extract. This difference in average size suggests that one or more additional chemical species in the extract are contributing to the reduction and stabilization of the Ag nanoparticles. A TLC separation of the ethanolic kudzu leaf extract showed two populations of molecules with retention factors of 0.30 and 0.36 (Fig. S15†). This result confirms that the ethanolic extract consists of more than chlorophyll.

To assess the chemical composition of the kudzu leaves and extracts beyond chlorophyll, we performed a series of phytochemical screening tests to determine if the following categories of molecules were present: reducing sugars, alkaloids, flavonoids, steroids, terpenoids, saponins and tannins (Fig. S16†). The raw kudzu leaves were found to contain reducing sugars, steroids and saponins. We note that alkaloids, flavonoids, terpenoids, and tannins may be present in the kudzu leaves, but are at lower concentrations, below the detection limit of the phytochemical test. Both aqueous and ethanolic extracts tested positive for the presence of reducing sugars and saponins. Table 1 summarizes the chemical profile of the raw kudzu leaves and extracts.

Extracts were further characterized with UV and IR absorption spectroscopy. UV absorption shows an electronic resonance at 265 nm that is present in both the aqueous and ethanolic extracts (Fig. 1), suggesting the species is soluble in both solvents. This excludes species such as carotenoids which are too hydrophobic to dissolve in water. Reducing sugars and saponins are soluble in ethanol and water, although the solubility of specific molecules in these categories may differ, and absorb UV light in the range of the resonances observed in the extract absorbance spectra below *ca.* 400 nm.[31–34] Further,

Table 1 Chemical profile for kudzu leaves and extract. The presence (+) or absence (–) is noted

	Leaf	Aqueous extract	Ethanolic extract
Chlorophyll	+	–	+
Reducing sugars	+	+	+
Alkaloids	–	–	–
Flavonoids	–	–	–
Steroids	+	–	–
Terpenoids	–	–	–
Saponins	+	+	+
Tannins	–	–	–

reducing sugars and saponins have been used to synthesize Ag nanoparticles in aqueous solutions.[43–49] Therefore, it is likely that these categories of phytochemicals are reducing and stabilizing agents in the aqueous extract and serve as co-reducing and co-stabilizing agents in the ethanolic extract of kudzu leaves.

FTIR spectra of the extracts were collected to look for further evidence of the presence of reducing sugars and saponins in kudzu leaf extracts (Fig. 7 and Table 2). A broad feature between *ca.* 3000 and 3500 cm^{-1} in both extracts is characteristic of O–H stretching from alcohol groups on reducing sugars. Additionally, peaks at 1733 and 1730 cm^{-1} in the ethanolic and aqueous extracts, respectively, are assigned to carbonyl stretches of ketones or aldehydes, prevalent functional groups in reducing sugars. Two C–O stretching modes are observed at 1375 (1379) and 1066 (1073) cm^{-1} in the ethanolic (aqueous) extract. We note that saponins contain sugar moieties, preventing definitive assignment of these vibrational modes to reducing sugars. Vibrational modes at 1606 and 1570 cm^{-1} in the aqueous and ethanolic extracts, respectively, may be attributable to C=C stretching modes of saponins.[49–51] Finally, prominent C–H stretching modes at 2847 cm^{-1} and 2918 cm^{-1} are observed in the ethanolic extract, likely from the phytol chain of chlorophyll. Collectively, the phytochemical screening, UV and IR absorption features support the assertion that reducing sugars and saponins are present in both extracts and likely are serving in reducing and stabilizing roles in the synthesis of Ag nanoparticles.

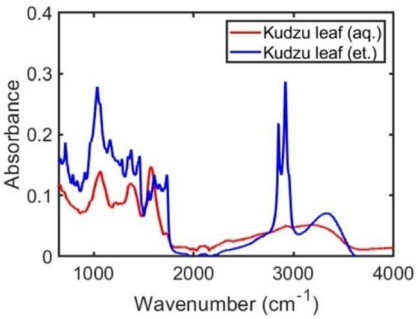

Fig. 7 FTIR absorbance spectra of solids from evaporated aqueous (red curve) and ethanolic (blue curve) kudzu leaf extracts.

Table 2 Potential functional group assignments for peaks observed in the FTIR spectra of ethanolic and aqueous kudzu leaf extracts

Observed peaks (cm^{-1})	Potential assignments
Ethanolic leaf extract	
1066	C–O stretch
1375	C–O stretch
1606	C=C stretch
1733	C=O stretch (ketone/aldehyde)
2847	C–H stretch
2918	C–H stretch
3000–3500	O–H stretch
Aqueous leaf extract	
1073	C–O stretch
1379	C–O stretch
1580	C=C stretch
1730	C=O stretch (ketone/aldehyde)
3000–3500	O–H stretch

An important aspect of controlling Ag nanoparticle size and morphology is the interaction of stabilizing ligands with the metal surface. As shown in Fig. 2, Ag nanoparticles support visible light localized surface plasmon resonances. One result of plasmon excitation by visible light is the generation of large electromagnetic fields localized to the surface of a nanoparticle, which has been exploited for enhancing spectroscopic signatures of molecules on or near the surface of a nanoparticle. When Ag nanoparticles are aggregated, the electromagnetic field intensifies, enabling the selective enhancement of spectroscopic signatures of surface molecules by many orders of magnitude.[52,53] To investigate the molecules present on the surface of Ag nanoparticles synthesized with kudzu leaf extracts, we performed surface-enhanced spectroscopy on clusters of aggregated Ag nanoparticles (see Experimental section).

First, we examined the surface-enhanced spectroscopic signals from Ag nanoparticles synthesized with ethanolic kudzu leaf extracts. A strong fluorescence signal was obtained with a peak wavelength of 675 nm, indicative of chlorophyll fluorescence (Fig. 8A).[54,55] Further, this signal showed a characteristic decay in intensity during continuous illumination, consistent with the photobleaching of a fluorophore. The control experiments using a chlorophyllin standard and using ethanolic extract in the presence and absence of light demonstrate that chlorophyll contributes to the reduction of Ag^+ in the formation of Ag nanoparticles, while the surface-enhanced fluorescence measurement indicates that chlorophyll is present on the nanoparticle surfaces and serves as a stabilizing agent. Surface-enhanced Raman scattering spectra (Fig. 9 and S17†) of Ag nanoparticles synthesized with ethanolic extract show several vibrational modes on the surface of these Ag nanoparticles, which are similar to those measured from the extract (Tables 2 and 3), indicating the presence of reducing sugars or saponins on the surface of the nanoparticles.

Surface-enhanced spectroscopic signals from Ag nanoparticles synthesized with aqueous kudzu leaf extract showed

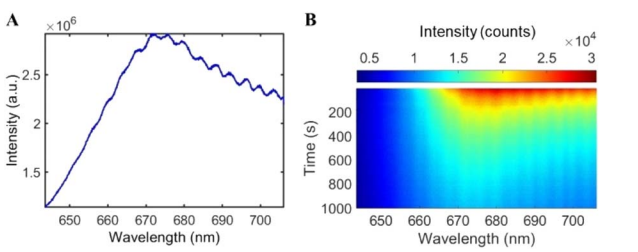

Fig. 8 (A) Surface-enhanced fluorescence from the surface of Ag nanoparticles synthesized with an ethanolic kudzu leaf extract indicating the presence of surface-bound chlorophyll. (B) Characteristic photobleaching of chlorophyll fluorescence under continuous light irradiation on the surface of Ag nanoparticles.

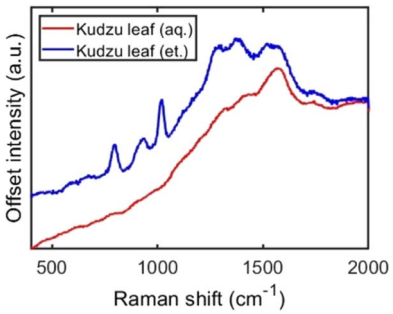

Fig. 9 Surface-enhanced Raman scattering from aggregated Ag nanoparticles synthesized with ethanolic (blue) and aqueous (red) kudzu leaf extracts.

Table 3 Potential functional group assignments for peaks observed in the surface-enhanced Raman scattering spectra from Ag nanoparticles synthesized with ethanolic and aqueous kudzu leaf extracts

Observed peaks (cm^{-1})	Potential assignments
Ethanolic leaf extract	
798	C–H bend
973	O–H bend
1019	C–O stretch
1288	C–O stretch
1384	C–O stretch
1521	C–O–H bend
1580	C=C stretch
1750	C=O stretch (carboxylic acid)
Aqueous leaf extract	
1580	C=C stretch
1750	C=O stretch (carboxylic acid)

vibrational modes at 1580 and 1750 cm^{-1}, tentatively assigned to C=C stretching and C=O stretching of carboxylic acids (Fig. 9), but fluorescence from chlorophyll was not detected (Fig. S18†). Of note is the mode with a carbonyl stretching contribution at 1750 cm^{-1}, consistent with the Ag nanoparticles synthesized with the ethanolic extract. A possible mechanism for the formation of Ag nanoparticles with aqueous kudzu leaf extracts is that the reducing sugars (containing an aldehyde or ketone, Fig. 7) transfer electrons and reduce Ag^+ to Ag^0 and, in the process, oxidize to form carboxylic acid sugars, which remain on the nanoparticle surface and serve as stabilizing ligands. This mechanism is also probable in the formation of Ag nanoparticles in the ethanolic extract and likely is occurring in competition with reduction and stabilization by chlorophyll.

Conclusions

In summary, we demonstrated the synthesis of Ag nanoparticles using kudzu extracts. Ethanolic kudzu leaf extracts formed smaller and more monodisperse Ag nanoparticles than aqueous extracts prepared from kudzu leaves or stems. Photoexcited chlorophyll extracted by ethanol was determined to play a pivotal role in the formation of small and monodisperse Ag nanoparticles, likely due to the enhanced reduction kinetics of Ag^+ and Ag nanoparticle stabilization by chlorophyll. Evidence for the presence of reducing sugars and saponins in aqueous and ethanolic extracts was presented. Reducing sugars and saponins are suspected to be the primary reducing and stabilizing agents in aqueous extracts and serve as co-reducing and co-stabilizing agents in the synthesis of Ag nanoparticles with ethanolic extracts. Further characterization of the chemical composition of the extracts is required to exhaust the possibilities of additional co-reducing and co-stabilizing agents. However, our control studies with chlorophyllin standards and syntheses carried out in the absence of light provide the support that chlorophyll extracted from plant species can be used to control the size and dispersity of biocompatible Ag nanoparticles. This study also opens up new green synthesis routes to control nanoparticle size by varying the concentration and photoexcitation of chlorophyll.

Author contributions

JFA collected kudzu samples, assisted in the design of experiments, performed kudzu extractions, conducted nanoparticle syntheses, characterized extracts and nanoparticles, analysed data and co-wrote the manuscript. AK performed kudzu extractions, conducted nanoparticle syntheses, characterized extracts and nanoparticles, determined phytochemical profiles, and measured surface-enhanced fluorescence and Raman scattering. MSA and FR performed X-ray diffraction measurements and analysis. HC assisted in the conception of the research. AJW conceived and supervised the project, assisted in experimental design, analysed data, and co-wrote the manuscript.

Conflicts of interest

There are no conflicts to declare.

Acknowledgements

The authors thank Dr Julia Aebersold and the Micro/Nano Technology Center for the collection of TEM images, Nathan Coleman for gathering the kudzu used for the experiments, and Johann Hemmer for assisting in figure preparation. This work was supported by funding from the Summer Research Opportunity Program (JFA) and start-up funding (AJW) from the University of Louisville.

References

1 V. K. Sharma, R. A. Yngard and Y. Lin, *Adv. Colloid Interface Sci.*, 2009, **145**, 83–96.
2 M. Ahamed, M. S. AlSalhi and M. K. J. Siddiqui, *Clin. Chim. Acta*, 2010, **411**, 1841–1848.
3 S. Kokura, O. Handa, T. Takagi, T. Ishikawa, Y. Naito and T. Yoshikawa, *Nanomed. Nanotechnol. Biol. Med.*, 2010, **6**, 570–574.
4 T. Gunasekaran, T. Nigusse and M. D. Dhanaraju, *Journal of the American College of Clinical Wound Specialists*, 2011, **3**, 82–96.

5 L. A. Austin, M. A. Mackey, E. C. Dreaden and M. A. El-Sayed, *Arch. Toxicol.*, 2014, **88**, 1391–1417.
6 C. A. Dos Santos, M. M. Seckler, A. P. Ingle, I. Gupta, S. Galdiero, M. Galdiero, A. Gade and M. Rai, *J. Pharm. Sci.*, 2014, **103**, 1931–1944.
7 N. Durán, M. Durán, M. B. de Jesus, A. B. Seabra, W. J. Fávaro and G. Nakazato, *Nanomed. Nanotechnol. Biol. Med.*, 2016, **12**, 789–799.
8 K. Jadhav, S. Deore, D. Dhamecha, R. H. R. S. Jagwani, S. Jalalpure and R. Bohara, *ACS Biomater. Sci. Eng.*, 2018, **4**, 892–899.
9 H. Chugh, D. Sood, I. Chandra, V. Tomar, G. Dhawan and R. Chandra, *Artif. Cells, Nanomed., Biotechnol.*, 2018, **46**, 1210–1220.
10 P. Mathur, S. Jha, S. Ramteke and N. K. Jain, *Artif. Cells, Nanomed., Biotechnol.*, 2018, **46**, 115–126.
11 S. H. Lee and B.-H. Jun, *Int. J. Mol. Sci.*, 2019, **20**, 865.
12 M. Rafique, I. Sadaf, M. S. Rafique and M. B. Tahir, *Artif. Cells, Nanomed., Biotechnol.*, 2017, **45**, 1272–1291.
13 S. Ahmad, S. Munir, N. Zeb, A. Ullah, B. Khan, J. Ali, M. Bilal, M. Omer, M. Alamzeb, S. M. Salman and S. Ali, *Int. J. Nanomed.*, 2019, **14**, 5087–5107.
14 C. Vanlalveni, S. Lallianrawna, A. Biswas, M. Selvaraj, B. Changmai and S. L. Rokhum, *RSC Adv.*, 2021, **11**, 2804–2837.
15 D. P. K. Lankveld, A. G. Oomen, P. Krystek, A. Neigh, A. Troost – de Jong, C. W. Noorlander, J. C. H. Van Eijkeren, R. E. Geertsma and W. H. De Jong, *Biomaterials*, 2010, **31**, 8350–8361.
16 M. van der Zande, R. J. Vandebriel, E. Van Doren, E. Kramer, Z. Herrera Rivera, C. S. Serrano-Rojero, E. R. Gremmer, J. Mast, R. J. B. Peters, P. C. H. Hollman, P. J. M. Hendriksen, H. J. P. Marvin, A. A. C. M. Peijnenburg and H. Bouwmeester, *ACS Nano*, 2012, **6**, 7427–7442.
17 M. Rai, A. Yadav and A. Gade, *Biotechnol. Adv.*, 2009, **27**, 76–83.
18 J. Y. Cheon, S. J. Kim, Y. H. Rhee, O. H. Kwon and W. H. Park, *Int. J. Nanomed.*, 2019, **14**, 2773–2780.
19 M. Pradeep, D. Kruszka, P. Kachlicki, D. Mondal and G. Franklin, *ACS Sustainable Chem. Eng.*, 2022, **10**, 562–571.
20 V. Venkatpurwar and V. Pokharkar, *Mater. Lett.*, 2011, **65**, 999–1002.
21 J. E. Hickman, S. Wu, L. J. Mickley and M. T. Lerdau, *Proc. Natl. Acad. Sci. U. S. A.*, 2010, **107**, 10115–10119.
22 I. N. Forseth and A. F. Innis, *Crit. Rev. Plant Sci.*, 2004, **23**, 401–413.
23 K. H. Wong, G. Q. Li, K. M. Li, V. Razmovski-Naumovski and K. Chan, *J. Ethnopharmacol.*, 2011, **134**, 584–607.
24 S. H. Eom, S.-J. Jin, H.-Y. Jeong, Y. Song, Y. J. Lim, J.-I. Kim, Y.-H. Lee and H. Kang, *Int. J. Mol. Sci.*, 2018, **19**, E1536.
25 O. A. Aiyegoro and A. I. Okoh, *BMC Compl. Alternative Med.*, 2010, **10**, 21.
26 Y. L. Chew, E. W. Ling Chan, P. L. Tan, Y. Y. Lim, J. Stanslas and J. K. Goh, *BMC Compl. Alternative Med.*, 2011, **11**, 12.
27 J. R. Shaikh and M. Patil, *Int. J. Chem. Stud.*, 2020, **8**, 603–608.
28 N.-U. Frigaard, K. L. Larsen and R. P. Cox, *FEMS Microbiol. Ecol.*, 1996, **20**, 69–77.
29 R. Croce and H. van Amerongen, *Nat. Chem. Biol.*, 2014, **10**, 492–501.
30 A. Sirohiwal, R. Berraud-Pache, F. Neese, R. Izsák and D. A. Pantazis, *J. Phys. Chem. B*, 2020, **124**, 8761–8771.
31 C. Sarazin, N. Delaunay, C. Costanza, V. Eudes, J.-M. Mallet and P. Gareil, *Anal. Chem.*, 2011, **83**, 7381–7387.
32 J. D. Oliver, M. Gaborieau, E. F. Hilder and P. Castignolles, *J. Chromatogr. A*, 2013, **1291**, 179–186.
33 W. A. Oleszek, *J. Chromatogr. A*, 2002, **967**, 147–162.
34 B. Roig and O. Thomas, *Anal. Chim. Acta*, 2003, **477**, 325–329.
35 Z. A. Ratan, M. F. Haidere, Md. Nurunnabi, S. Md. Shahriar, A. J. S. Ahammad, Y. Y. Shim, M. J. T. Reaney and J. Y. Cho, *Cancers*, 2020, **12**, 855.
36 M. K. Temgire and S. S. Joshi, *Radiat. Phys. Chem.*, 2004, **71**, 1039–1044.
37 M. R. Bindhu and M. Umadevi, *Spectrochim. Acta, Part A*, 2015, **135**, 373–378.
38 A. S. Ethiraj, S. Jayanthi, C. Ramalingam and C. Banerjee, *Mater. Lett.*, 2016, **185**, 526–529.
39 C. S. Gibbons and J. Trotter, *J. Chem. Soc. A*, 1971, 2058–2062.
40 P. Meyer, A. Rimsky and R. Chevalier, *Acta Crystallogr., Sect. B: Struct. Crystallogr. Cryst. Chem.*, 1976, **32**, 1143–1146.
41 P. Meyer, A. Rimsky and R. Chevalier, *Acta Crystallogr., Sect. B: Struct. Crystallogr. Cryst. Chem.*, 1978, **34**, 1457–1462.
42 G. H. Krause and E. Weis, *Annu. Rev. Plant Physiol. Plant Mol. Biol.*, 1991, **42**, 313–349.
43 A. Panáček, L. Kvítek, R. Prucek, M. Kolář, R. Večeřová, N. Pizúrová, V. K. Sharma, T. Nevěčná and R. Zbořil, *J. Phys. Chem. B*, 2006, **110**, 16248–16253.
44 J. Huang, G. Zhan, B. Zheng, D. Sun, F. Lu, Y. Lin, H. Chen, Z. Zheng, Y. Zheng and Q. Li, *Ind. Eng. Chem. Res.*, 2011, **50**, 9095–9106.
45 R. Dondi, W. Su, G. A. Griffith, G. Clark and G. A. Burley, *Small*, 2012, **8**, 770–776.
46 S. Durmazel, A. Üzer, B. Erbil, B. Sayın and R. Apak, *ACS Omega*, 2019, **4**, 7596–7604.
47 R. Geethalakshmi and D. V. L. Sarada, *Ind. Crops Prod.*, 2013, **51**, 107–115.
48 Y. Choi, S. Kang, S.-H. Cha, H.-S. Kim, K. Song, Y. J. Lee, K. Kim, Y. S. Kim, S. Cho and Y. Park, *Nanoscale Res. Lett.*, 2018, **13**, 23.
49 R. Segura, G. Vásquez, E. Colson, P. Gerbaux, C. Frischmon, A. Nesic, D. E. García and G. Cabrera-Barjas, *J. Sci. Food Agric.*, 2020, **100**, 4987–4994.
50 M. S. Almutairi and M. Ali, *Nat. Prod. Res.*, 2015, **29**, 1271–1275.
51 S. Peng, Z. Li, L. Zou, W. Liu, C. Liu and D. J. McClements, *Food Funct.*, 2018, **9**, 1829–1839.
52 K. Kneipp, Y. Wang, H. Kneipp, L. T. Perelman, I. Itzkan, R. R. Dasari and M. S. Feld, *Phys. Rev. Lett.*, 1997, **78**, 1667–1670.
53 E. C. Le Ru, E. Blackie, M. Meyer and P. G. Etchegoin, *J. Phys. Chem. C*, 2007, **111**, 13794–13803.
54 G. H. Krause and E. Weis, *Photosynth. Res.*, 1984, **5**, 139–157.
55 R. Pedrós, I. Moya, Y. Goulas and S. Jacquemoud, *Photochem. Photobiol. Sci.*, 2008, **7**, 498–502.